

Development of a thulium (Tm:YAP) laser system for brain tissue ablation

Temel Bilici · Sevinc Mutlu · Hamit Kalaycioglu ·
Adnan Kurt · Alphan Sennaroglu · Murat Gulsoy

Received: 19 November 2010 / Accepted: 17 March 2011 / Published online: 12 April 2011
© Springer-Verlag London Ltd 2011

Abstract In this study, a thulium (Tm:YAP) laser system was developed for brain surgery applications. As the Tm:YAP laser is a continuous-wave laser delivered via silica fibers, it would have great potential for stereotaxic neurosurgery with highest local absorption in the IR region. The laser system developed in this study allowed the user to set the power level, exposure time, and modulation parameters (pulse width and on-off cycles). The Tm:YAP laser beam (200–600 mW, 69–208 W/cm²) was delivered from a distance of 2 mm to cortical and subcortical regions of ex-vivo Wistar rat brain

tissue samples via a 200-μm-core optical fiber. The system performance, dosimetry study, and ablation characteristics of the Tm:YAP laser were tested at different power levels by maximizing the therapeutic effects and minimizing unwanted thermal side-effects. The coagulation and ablation diameters were measured under microscope. The maximum ablation efficiency (100 × ablation diameter/coagulation diameter) was obtained when the Tm:YAP laser system was operated at 200 mW for 10 s. At this laser dose, the ablation efficiency was found to be 71.4% and 58.7% for cortical and subcortical regions, respectively. The fiber-coupled Tm:YAP laser system is hence proposed for the delivery of photo-thermal therapies in medical applications.

T. Bilici · M. Gulsoy
Biophotonics Laboratory, Institute of Biomedical Engineering,
Boğaziçi University,
Kandilli Kampus,
Cengelkoy 34684 Istanbul, Turkey

S. Mutlu
Instituto Gulbenkian de Ciência,
Oeiras 2781-901, Portugal

H. Kalaycioglu
Institute of Material Science and Nanotechnology,
Bilkent University,
Cankaya 06800 Ankara, Turkey

A. Kurt
Teknofil Ltd. Sti., Zekeriyaköy,
Sarıyer 34450 Istanbul, Turkey

A. Sennaroglu
Laser Research Laboratory, Department of Physics,
Koç University,
Sarıyer 34450 Istanbul, Turkey

M. Gulsoy (✉)
Institute of Biomedical Engineering, Boğaziçi University,
Kandilli Kampus,
Cengelkoy 34684 Istanbul, Turkey
e-mail: gulsoy@boun.edu.tr

Keywords Thulium laser · 1980-nm · Brain tissue ablation · Ablation efficiency

Introduction

There has been a growing interest in lasers emitting in the 2-μm region since they can be used in numerous biophotonics applications. One group of sources for 2-μm laser radiation includes solid-state gain media doped with thulium (Tm³⁺) ions. When pumped at wavelengths around 780–795 nm, Tm³⁺-doped crystals fluoresce around 1.8–2.0 μm. One particular example for Tm³⁺-doped crystals is the thulium-doped yttrium aluminum perovskite (Tm:YAP) crystal [1, 2]. Here, the concentration of Tm³⁺ ions influences the absorbance, fluorescence lifetime, and the optical gain of the Tm:YAP laser [3]. In addition, sufficiently high Tm³⁺ concentrations may further lead to an increase in the population inversion for the ³F₄ → ³H₆ transition (between 1.9 μm and 2 μm) via the cross-relaxation process (³H₄, ³H₆) → (³F₄, ³F₄) [4, 5]. As such,

the self-quenching mechanism of the Tm:YAP laser between $^3\text{H}_4$ and $^3\text{F}_4$ levels produces two excited photons in the upper laser level for one absorbed pump photon, which can potentially make the Tm:YAP laser very efficient [6]. One additional advantage is that the 4-nm-wide absorption band of Tm:YAP is broader compared to that of Tm:YAG. This results in a better tolerance to wavelength drifts in the pump diodes. In Tm:YAP, the absorption band corresponding to the optical transition between $^3\text{H}_6$ and $^3\text{H}_4$ levels at 795 nm can be easily pumped by high-power AlGaAs lasers diodes. The wide availability of 800-nm pump diodes further makes the development of thulium lasers much easier in contrast to holmium lasers, which require in-band pumping near 2 μm .

Laser emission from Tm:YAP is observed over the range 1.86–2.03 μm with different efficiencies that depend on the output coupler transmission, ion concentration, and losses [7, 8]. The output wavelength is determined by the amount of loss due to reabsorption from the ground state, which increases as the laser wavelength decreases. Therefore, the Tm:YAP laser can be designed to operate at shorter wavelengths by using higher output coupler transmission. In the Tm:YAP laser, the reabsorption loss is proportional to the ground state population, the crystal length, and Tm^{3+} concentration. In addition, the wavelength of the thulium lasers can be tuned between 1,845 nm and 1,995 nm by using intracavity wavelength-selective filters such as birefringent plates and prisms [9].

In the literature, there is a wide range of applications of 2- μm lasers in tissue ablation. The ablation rates and tissue effects produced by a pulsed holmium laser with a wavelength of 2.12 μm and a pulsed thulium laser with a wavelength of 2.01 μm were compared in vitro and the thulium laser was found to yield a significantly lower threshold of ablation with far less residual thermal injury. The zone of residual thermal injury produced with the thulium laser was found to be slightly less than that produced by the holmium laser [10]. In addition, the cw thulium laser was used in the enucleation of the prostate with no collateral damage to adjacent tissue [11]. Neuro-endoscopy study with a 2.0- μm near-infrared (NIR) laser system was also performed [12].

Lasers in neurosurgery provided precise tumor ablation by making spherical lesions without carbonizing. Brain tissue ablation has been investigated with different laser sources, such as 2.0- μm NIR laser [12], CO_2 , KTP, argon lasers, Nd:YAG lasers, 980-nm diode lasers [13], and 2.94- μm Er:YAG [14] lasers, as alternative tools to conventional electrosurgical units. The CO_2 laser was not found to be suitable for coagulating blood vessels but they were reported to be good tools for cutting brain tissue [13]. The Nd:YAG laser at 1,064 nm was used for coagulating both brain tissue and blood vessels, however, due to its high scattering and poor

absorption, adjacent tissues were thermally altered as also seen in KTP and argon laser applications [14]. By histological examinations, minimal thermal damage of nearby tissue was reported for the 980-nm diode lasers. Cavitation effects as a result of the explosive ablation process were also observed in the Er:YAG laser application. In this study, a Tm:YAP laser system is employed for ablation applications due to the strong absorption of its output radiation in water. The Tm:YAP laser at 1.98 μm has a stronger absorption coefficient in liquid water than that for Tm:YAG and Ho:YAG lasers, around 2 μm [15]. Although lasers near 3 μm have the highest absorption in biological tissue due to the overlap with the fundamental O-H vibrational resonance of water, silica fibers are not transparent at wavelengths longer than 2 μm and delivery with conventional low-cost fiber-optic cables is difficult. In contrast, the Tm:YAP laser at 1.98 μm can be readily coupled to conventional low-OH silica fibers unlike longer-wavelength lasers such as CO_2 lasers (10.6 μm) [16].

The aim of this study is to develop a Tm:YAP-based laser system for brain tissue ablation. The ablation efficiency ($100 \times \text{ablation diameter/coagulation diameter}$) of the developed laser system was experimentally tested on brain tissue ex-vivo as a predosimetry ablation study. Thermal changes were quantified in terms of ablation efficiency.

Materials and methods

The Tm:YAP laser system

The Tm:YAP laser system developed for laser tissue applications includes a Tm:YAP laser resonator setup, diode laser driver, water chiller, modulation controller unit, and acquisition/control software.

Tm:YAP laser resonators can be designed by using high-power pump diodes near 800 nm that overlap with the absorption band of the Tm:YAP crystal at 795 nm. The power performance of Tm:YAP lasers is affected by the doping concentration Tm^{3+} ions inside the YAP crystal. Varying the active ion concentration can change the strength of cross relaxation, reabsorption losses, and non-radiative decay rates. Previous spectroscopic measurements and rate-equation analysis suggest that cross relaxation should be effective in samples with 1.5% Tm^{3+} ion concentration [9]. Therefore, a cylindrical 1.5% Tm^{3+} doped Tm:YAP crystal (Crytur, Inc., diameter: 5 mm, length: 4 mm), was used to obtain optical gain inside the laser resonator. The crystal was normal cut and both faces had antireflection coatings near 1,940 nm [17].

The schematic of the laser resonator setup is shown in Fig. 1. The resonator consisted of a flat input mirror and a

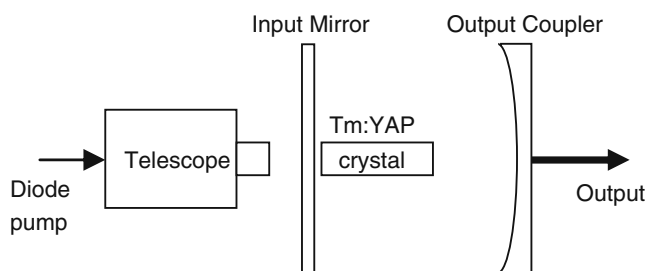


Fig. 1 Experimental setup of Tm:YAP laser resonator. The laser output was coupled to a 200- μm -core fiber ($\text{NA}=0.22$). The maximum output power of 1.14 ± 0.2 W ($395\text{ W}/\text{cm}^2$) was obtained from a 2-mm distance

curved output coupler with a radius of 10 cm. The input mirror was reflective around $1.94\text{ }\mu\text{m}$ and transmitting at 795 nm. The Tm:YAP crystal, which was positioned near the input mirror, was wrapped in indium foil and held between copper holders maintained at $20\pm2^\circ\text{C}$ by water cooling. The length of the resonator was 7.5 cm. The Tm:YAP resonator was end-pumped with a fiber-coupled laser diode at 797 nm (maximum operational power of 10 W). An imaging telescope was used to focus the pump beam inside the crystal. The output laser radiation was coupled to a 200- μm -core fiber ($\text{NA}=0.22$) by a converging lens. The output beam characteristics M^2 was measured as 22.7 by knife-edge technique. The fiber output spot size and average light intensity of the Tm:YAP laser were analyzed with respect to the distance to target tissue.

The controller unit that was employed to operate the laser consisted of five blocks [18]: (1) a microcontroller unit, (2) an analog-to-digital converter, (3) an RS 232 serial communication unit, (4) a digital-to-analog converter, and (5) a relay controller switching unit. (1) In the microcontroller unit, an 8-bit microcontroller PIC16C84 (Burr Brown, Texas Instruments, TX) was used. The control software developed in assembly language was compiled and loaded into PIC16C84 in MPLAB Integrated Development Environment (Microchip Technology Inc., AZ). The application software processes data received from the diode laser power supply and user interface program, while the microcontroller waits for commands from the user interface by checking the diode laser status. (2) The analog-to-digital converter block converts the analog signals of the diode current and diode temperature values to digital signals to be processed by the microcontroller. For the analog-to-digital conversion, a four-channel, 16-bit sampling converter (ADS7825 IC; Burr Brown, Texas Instruments, TX) was used with $\pm 10\text{ V}$ input range for each channel with a resolution of $305\text{ }\mu\text{V}/\text{bit}$. (3) The RS-232 serial communication unit enabled the microcontroller unit to communicate with a PC by performing asynchronous communication in RS-232 communication protocol (developed by the Electronic Industries Association, South

Australia, EIA232). As a multi-channel RS-232 driver/receiver with two receive-transmit channel pairs, MAX232 IC (Maxim Integrated Products, CA) was used via a serial port of the PC. Half-duplex RS232 serial communication mode was implemented by setting the baud rate to 9600 bps. (4) A digital-to-analog converter (DAC714 IC, Burr Brown, Texas Instruments, TX) was used to convert digital signals taken from the user interface program to analog signal in order to set the diode laser current in the laser power supply. (5) The relay-controlled switching unit has four independent relays that can be activated by the user for complete galvanic power isolation.

The acquisition and control software was developed in Labview 6.0 (National Instruments, TX) programming environment. The data flow and all units of the controller circuit were controlled by subprograms in the user interface. All the subprograms were then combined into one main user interface according to the algorithm of the laser operation. Both continuous and modulated laser output with different parameters was provided by the user interface software. The user interface program communicates with the laser diode via the controller circuit in order to set the operating parameters of the laser including power, duration, and pulsed mode cycles. The user can switch on and off the laser and set the diode current to attain the desired power level and duration of operation with a particular duty cycle (20-Hz maximum). In the pulsed mode of operation, the controller communicates with the laser diode and switches the diode current on and off as a square wave (off-cycle, on-cycle, and number of cycles).

Ablation experiments on ex vivo brain tissue with the Tm:YAP laser system

The first experiments were aimed at investigation of dosimetry levels of Tm:YAP laser system for brain tissue ablation applications. In previously performed in-vitro trials, it was observed that the Tm:YAP laser radiation was mostly absorbed at the surface of the tissues. Thermal alterations (coagulation, ablation, and carbonization) led to changes in thermal and optical properties of the tissue at the surface and this changed the thermal penetration inside the tissue. In addition, increasing the laser power increased the thermally altered areas and penetration depths. By increasing the average light intensity (W/cm^2) of the laser system, the thermal and carbonization side-effects were observed even in shorter time durations (200 ms).

The ex-vivo coronal brains were sliced in 4–5 mm samples. The Tm:YAP laser was applied from a distance of 2 mm to cortical (grey matter) and subcortical (white matter) regions of the tissue samples on a vertical translational platform. Different exposure durations were applied to compare the thermal effects. The selected Tm:

YAP laser doses (laser power, average light intensity, and duration) were determined from the efficient results obtained in previously performed in-vitro studies. The Tm:YAP laser doses and the sample sizes are tabulated in Table 1.

The total coagulation diameter (CD) and ablation diameter (AD) of each sample (Fig. 2) were measured under a light microscope (Eclipse 80i, Nikon Co., Tokyo, Japan). Measurements were performed using Imaging Software (NIS Elements-D, Nikon Co., Tokyo, Japan). The ablation efficiency (AE) was determined from $AE = 100 \times AD/CD$. All data were expressed as mean \pm standard deviation. The data were analyzed by ANOVA test, where a value of $p < 0.05$ is considered to be statistically significant.

Results

Tm:YAP laser system output

The power measurements at different diode currents were measured by a power meter (Newport 1918C, IL, USA) while the Tm:YAP crystal and pumping diode laser were water chilled at $20 \pm 2^\circ\text{C}$ by a chiller (Polyscience MiniChiller 5005, CA, USA). The maximum standard deviation of power measurements were found as 0.01 W, which showed high stability and reproducibility of power levels of the Tm:YAP laser. The laser spot size and the average light intensity on the target tissue were measured by using M^2 method. The fiber output spot size of the Tm:YAP laser changes with respect to the distance to target tissue and this makes the average light intensity different for each distance (Fig. 3). The laser was applied from 2 mm distance in the experiments in this study, and the laser spot diameter was measured from this distance as 0.6 mm.

Ablation of cortical and subcortical tissues by the Tm:YAP laser at 200 mW

Coagulation and ablation diameters of both cortical and subcortical samples exposed to 200 mW Tm:YAP laser are given in Fig. 4a. There is no statistically significant

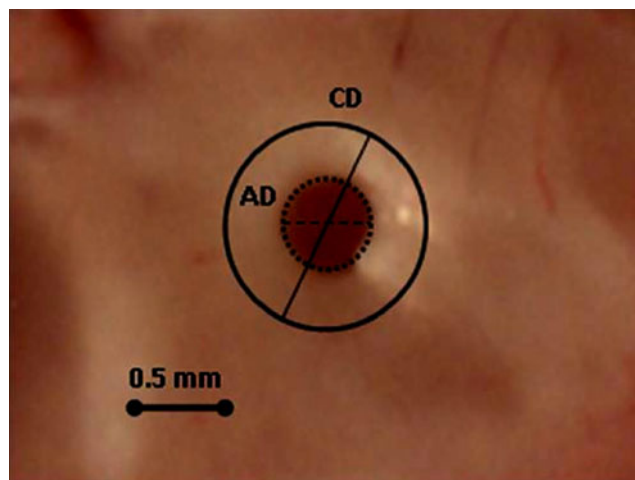


Fig. 2 A brain tissue sample exposed to Tm:YAP laser. CD shows the coagulation diameter and AD shows the ablation diameter

difference between coagulation diameters of cortical and subcortical samples at 3 s ($p = 0.98$), 6 s ($p = 1.7$), and 10 s ($p = 0.5$) of laser exposure. However, at 15-s application, coagulation diameters were statistically significant ($p < 0.01$) among cortical and subcortical samples. There were statistically significant ablation diameters found only at 10-s ($p = 0.037$) and 15-s ($p = 0.04$) exposure among cortical and subcortical samples.

For cortical tissue samples, the increase in laser application duration from 3 to 6 s and from 6 to 10 s did not differentiate the coagulation diameter statistically ($p = 0.31$). However, at the 15-s application, differentiated the coagulation diameter statistically ($p < 0.01$). Increase in laser application duration increased the ablation diameters, which are statistically significant among 3-s and 6-s applications ($p = 0.0025$), among 6-s and 10-s applications ($p = 0.024$). There was no statistical significance for ablation diameters among 10-s and 15-s laser applications ($p = 0.06$). For subcortical tissue applications, the increase in duration from 3 to 6 s increased the coagulation diameter ($p = 0.053$). The duration increase from 6 to 10 s ($p = 0.006$) and from 10 to 15 s ($p < 0.000$) provided statistically significant coagulation diameters.

Table 1 Tm:YAP laser dosimetry levels applied to ex vivo brain tissues for ablation analysis

Zone	Laser power	Average light intensity	Duration (number of samples)
Cortical	200 mW	69 W/cm ²	3 s ($n=13$), 6 s ($n=8$), 10 s ($n=10$), 15 s ($n=24$)
Cortical	400 mW	139 W/cm ²	1 s ($n=8$), 3 s ($n=15$), 6 s ($n=16$)
Cortical	600 mW	208 W/cm ²	1 s ($n=8$), 3 s ($n=12$), 6 s ($n=10$)
Subcortical	200 mW	69 W/cm ²	3 s ($n=8$), 6 s ($n=8$), 10 s ($n=13$), 15 s ($n=12$)
Subcortical	400 mW	139 W/cm ²	1 s ($n=8$), 3 s ($n=13$), 6 s ($n=8$)
Subcortical	600 mW	208 W/cm ²	1 s ($n=8$), 3 s ($n=11$), 6 s ($n=8$)

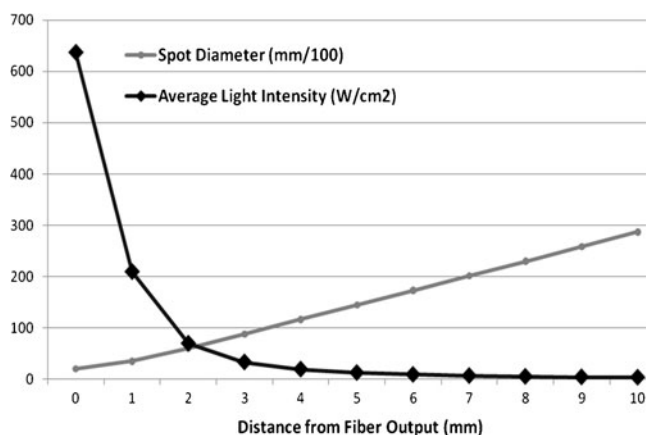


Fig. 3 The spot diameter (mm/100) and the average light intensity (W/cm^2) of the Tm:YAP laser output when the laser output power is 200 mW

Ablation of cortical and subcortical tissues by the Tm:YAP laser at 400 mW

Coagulation and ablation diameters of both cortical and subcortical samples exposed to 400-mW output of the Tm:YAP laser are given in Fig. 4b. Since the average light intensity at 400 mW was much higher, the experiments were performed from 1-s application duration to 6-s application duration until the carbonization effect was observed. Coagulation effects were observed even at 1-s exposure.

Among cortical and subcortical tissue samples, coagulation diameter for subcortical samples was statistically higher ($p = 0.03$) than coagulation diameter for cortical samples at 6-s application. Ablation diameters were not found to be statistically significant among cortical and subcortical samples at 1-s ($p = 0.92$), 3-s ($p = 0.08$), and 6-s ($p = 0.06$).

For both cortical and subcortical tissue samples, increasing the duration from 3 to 6 s made the coagulation diameters higher and statistically significant ($p = 0.03$). On the other hand, ablation diameters were found to be higher and statistically significant when the application duration was increased from 1 to 3 s ($p = 0.024$) for subcortical samples. For cortical samples, increasing application duration from 1 to 6 s at 400 mW, made ablation diameters statistically significant ($p = 0.008$).

Ablation of cortical and subcortical tissues with the Tm:YAP laser at 600 mW

Coagulation and ablation diameters of both cortical and subcortical samples exposed to 600 mW Tm:YAP laser are given in Fig. 4c. At the laser power of 600 mW, there were no statistically significant coagulation and ablation diameters among cortical and subcortical samples.

For cortical samples, coagulation diameters among 3-s and 6-s durations were found statistically significant ($p = 0.01$). On the other hand, ablation diameters were not found statistically significant among 1-s and 6-s durations ($p = 0.32$), among 3-s and 6-s durations ($p = 0.25$), and among 1-s and 6-s durations ($p = 0.84$). For subcortical samples, increasing the duration from 3 to 6 s made the coagulation diameter higher and statistically significant ($p = 0.02$). Ablation diameters were not found to be statistically significant from 1-s to 3-s durations ($p = 0.12$), from 3-s to 6-s durations ($p = 0.24$).

The coagulation and ablation diameters found in the experiments were used to calculate the ablation efficiency for each Tm:YAP laser power level. Ablation efficiencies are shown in Fig. 5 for 200-mW, 400-mW, and 600-mW power levels.

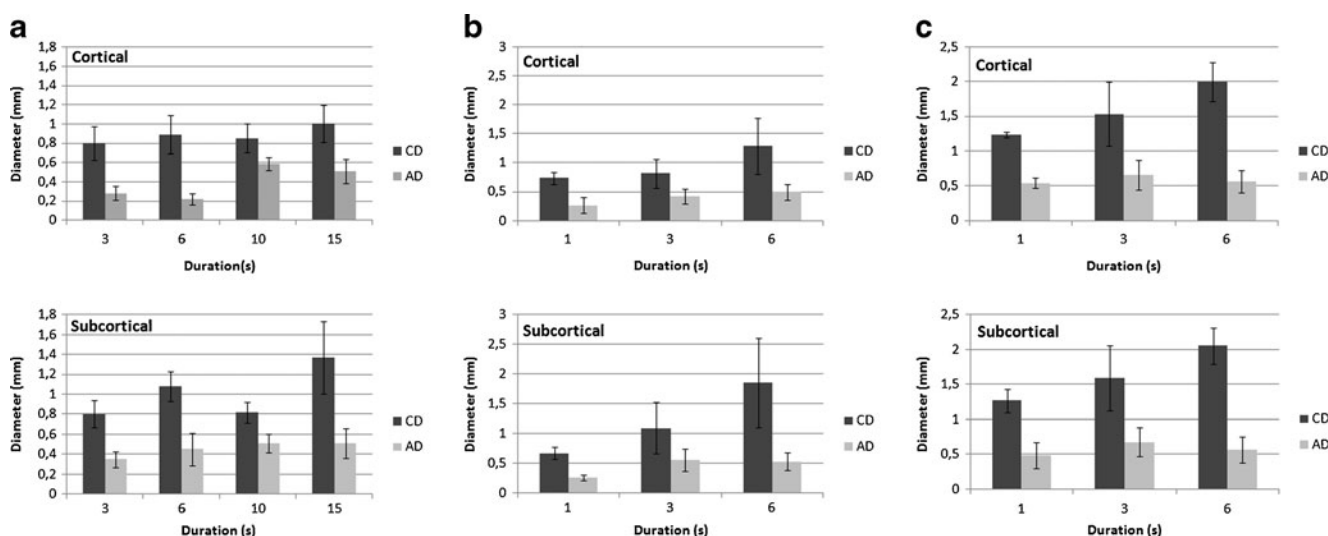


Fig. 4 Coagulation and ablation diameters of cortical and subcortical brain tissue exposed to Tm:YAP laser at 200 mW (a), 400 mW (b), and 600 mW (c)

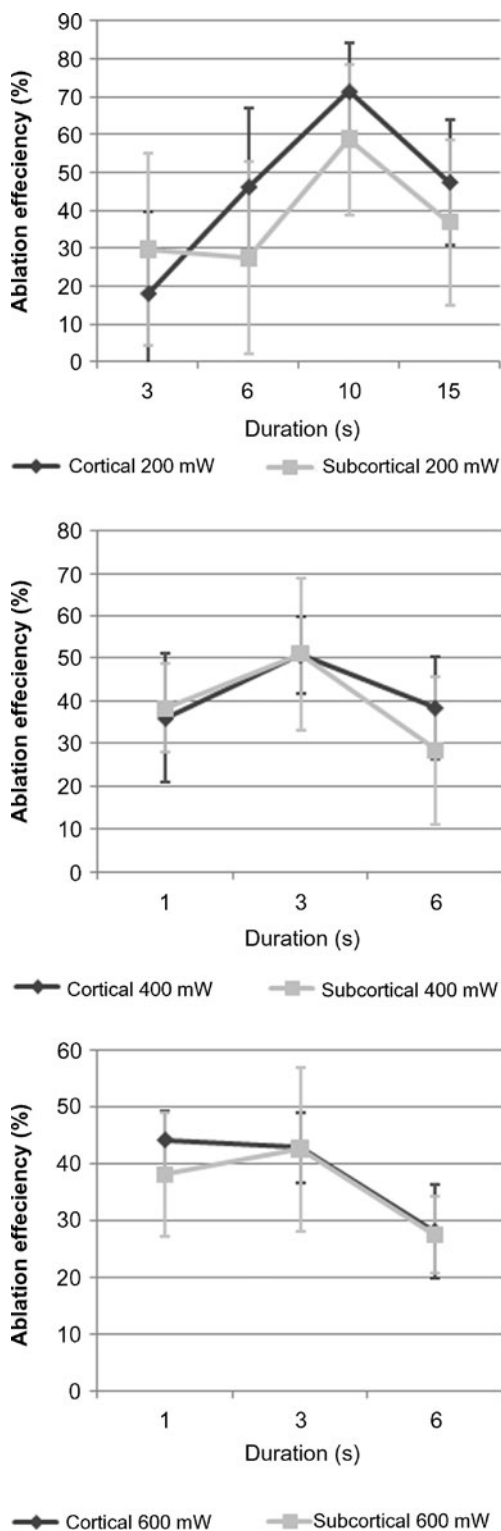


Fig. 5 Ablation efficiencies of cortical and subcortical brain tissues exposed Tm:YAP laser at 200-mW, 400-mW, and 600-mW of output power

The maximum ablation efficiency was obtained at 200 mW/10 s of Tm:YAP laser application for both cortical and subcortical tissues. At 400-mW Tm:YAP application, the duration of 3 s provided the highest ablation efficiency

at 400 mW, however, it was lower than the maximum ablation efficiency at 200 mW. At 600-mW application, changing durations did not possess statistically significant ablation efficiencies. As a result, the maximum ablation efficiency was obtained at 200 mW Tm:YAP laser application for a duration of 10 s for both cortical and subcortical brain tissues.

Discussion

Laser tissue interactions are thermal and highly nonlinear time-varying dynamic processes [19]. Photothermal interactions result from the transformation of absorbed light energy into heat. The heat deposition in tissues by laser application is strongly dependent on optical tissue properties like scattering and absorption as well as thermal properties. The optical absorption coefficient strongly depends on the wavelength of the laser radiation applied. The heat storage and transfer are also dependent on thermal tissue properties, such as heat capacity and thermal conductivity. The interaction of a laser light with tissue, therefore, depends on the wavelength of the laser, exposure time, and the optical properties of the tissue, which are determined by the structure, water content, blood circulation, heat conductivity, heat capacity, and density of tissue. However, optical and thermal properties of tissue are not constant and change during laser irradiation. Thermal conductivity is decreased due to dehydration and heat diffusion is consequently reduced and tissue temperature is increased. Depending on the duration and peak value of the temperature achieved, different effects like coagulation, vaporization, melting or carbonization may be observed. The temperature rise leads to protein dehydration, denaturation, coagulation, and/or ablation [20].

In tissue ablation, the aim is to remove the target tissue with minimal thermal damage to the surrounding tissue. Energy is dissipated primarily close to the tissue surface. Once the tissue surface is broken, the ablation spreads in deeper layers of the tissue. For deeper layers, propagation of thermal energy is reduced to the edge of the dehydrated zone [21].

The 2- μ m lasers suggest the potentials for accurate tissue removal by thermally induced coagulative and hemostatic effects. Water is the primary absorbing component in tissue at wavelengths above 1.4 μ m, leading to efficient conversion of light into heat. Longer infrared wavelengths heat the surface layer of water on the irradiated tissue, with subsequent heat conduction to the tissue elements below this surface. As water is removed from the tissue, local thermal conductivity decreases. This results in reduced heat conduction to the surrounding area.

The water absorption at 1,980 nm is 89 cm^{-1} . The optical penetration depth of 2- μ m lasers was found to be about

300 μm [22]. However, water absorption around 2 μm is strongly temperature-dependent and tissue ablation is a highly temperature dynamic process. At wavelengths between 1.85 and 2.15 μm , the absorption coefficient decreases substantially as temperature increases [23]. To avoid the thermal damage and carbonization of the target tissue, controlling the laser parameters and dosimetry studies are very crucial.

The surgical Tm:YAP laser system was developed in this study and the system produced laser beams with adjustable parameters by communicating accurately with the user interface program. Users can adjust the power and laser duration in on/off cycles. Controlling the mode of operation can change the photothermal effect on soft tissue. Before any clinical applications, the dosimetry study can be performed in terms of power, duration, and modulation parameters. Depending on the laser parameters, the dimension of the thermally altered areas is changed from coagulation to carbonization. Diameters of lesions increase with increasing power and duration. The system performance and ablation characteristics were tested on Wistar rat brain tissue *ex vivo* with different power levels of the Tm:YAP laser.

The Tm:YAP laser system at 2 μm was designed to be operational in both continuous-wave and pulsed modulation modes. The ablation characteristics of brain and Tm:YAP laser interactions are worth being performed in future studies to maximize the ablation efficiency since thermal injury of surrounding tissues was minimized by using pulsed radiation due to cooling of the tissue between pulses [24]. When the laser pulse width was less than the tissue thermal relaxation time, thermal diffusion outside the application area was reduced and the thermal injury of the surrounding tissues was minimized. In addition, the instrumentation and dosimetry study presented here can be expanded with histological examination in order to understand the limits of the thermal effects that the laser system creates.

Around 2- μm wavelengths, lasers coupled through a fiber offer good coagulation properties. At higher wavelengths, like Er:YAG and CO₂ lasers, lasers offer similar coagulation properties with high absorption by water as 2- μm lasers; however, the optimization of fiber delivery of Er:YAG and CO₂ lasers is difficult in clinical use [25]. Therefore, the Tm:YAP laser system is also promising for tissue welding applications [26] and stimulates body sites for laser somatosensory evoked potentials (LSEP) [27].

This study can contribute to a variety of medical applications in design and characterization of Tm:YAP laser system for delivering thermal therapies. The experiments suggest an efficient starting point for a clinical dosimetry study for brain tissue ablation. Further experiments should be performed on higher animals in order to bring this technique to clinical practice. The ablation efficiency can be further increased by optimizing the laser pulse duration and energy

density for each kind of biological tissue through histology studies.

Conclusions

In this study, a new Tm:YAP surgical laser system was developed. The system performance and ablation characteristics of the laser system were performed by sampled *ex vivo* experiments on Wistar rat brain tissue. Optimization of the Tm:YAP laser ablation efficiency for cortical and subcortical brain tissues was performed by maximizing the therapeutic effect and minimizing unwanted side-effects with different power levels of the Tm:YAP laser. The maximum ablation efficiency was obtained when the Tm:YAP laser was applied at the power level of 200 mW with a duration of 10 s (2 J). At this laser dose, the ablation efficiency was obtained as 71.4% for cortical region and 58.7% for subcortical region. The fiber-coupled Tm:YAP laser system was found to be promising for photo-ablation applications. Further investigation of Tm:YAP laser applications has been warranted.

Acknowledgements This work was supported by the Scientific and Technological Research Council of Turkey under TUBITAK-107E119 grant to Murat Gulsoy, Ph.D and under Bogazici University Scientific Research Fund BAP1952. The authors thank Resit Canbeyli, Ph. D., for providing the environment to perform *in vivo* experiments in the Psychobiology Laboratory, Bogazici University. A. Sennaroglu further acknowledges the research support provided by the Turkish Academy of Sciences. T. Bilici would like to thank Ozgur Tabakoglu, Nermin Topaloglu, Ayse Sena Sarp, and Eray Sevingil.

References

1. Elder IF, Payne J (1997) Diode-pumped, room-temperature Tm:YAP laser. *Appl Opt* 36:8606–8610
2. Li Y, Yao B, Wang Y, Ju Y, Zhao G, Zong Y, Xu J (2007) High efficient diode-pumped Tm:YAP laser at room temperature. *Chin Opt Lett* 5:286–287
3. Ni H, Rand SC (1991) Avalanche upconversion in Tm:YALO₃. *Opt Lett* 16:1424
4. Cornacchia F, Parisi D, Bernardini C, Toncelli A, Tonelli M (2004) Efficient, diode-pumped Tm³⁺:BaY₂F₈ vibronic laser. *Opt Express* 12:1982–1989
5. Razdobreev I, Shestakov A (2006) Self-pulsing of a monolithic Tm-doped YAlO₃ microlaser. *Phys Rev A* 73:053815
6. Elder IF, Payne MJP (1998) Lasing in diode-pumped Tm:YAP, Tm, Ho:YAP and Tm, Ho:YLF. *Opt Commun* 145:329–339
7. Stoneman RC, Esterowitz L (1995) Efficient 1.94- μm Tm:YALO laser. *IEEE J Sel Top Quantum Electron* 1:78–82
8. Elder IF, Payne J (1998) Diode-pumped, room-temperature Tm:YAP laser. *Appl Opt* 36:8606–8610
9. Kalaycioglu H, Sennaroglu A (2008) Low-threshold continuous-wave Tm³⁺:YAlO₃ laser. *Opt Commun* 281:4071–4074
10. Nishioka NS, Domankevitz Y (1990) Comparison of tissue ablation with pulsed holmium and thulium lasers. *IEEE J Quantum Electron* 26:2271–2275

11. Gordon S, Watson G (2006) Thulium laser enucleation of the prostate. *Eur Urol Suppl* 5:310
12. Ludwig HC, Kruschat T, Knobloch T, Teichmann HO, Rostasy K, Rohde V (2007) First experiences with a 2.0- μ m near infrared laser system for neuroendoscopy. *Neurosurg Rev* 30:195–201
13. Bozkulak O, Tabakoglu HO, Aksoy A, Kurtkaya O, Sav A, Canbeyli R, Gulsoy M (2004) 980-nm diode laser for brain surgery: histopathology and recovery period. *Lasers Med Sci* 19:41–47
14. Gulsoy M, Celikel TA, Kurt A, Canbeyli R, Çilesiz I (2001) Er: YAG Laser ablation on cerebellar and cerebral tissue. *Lasers Med Sci* 16:40–43
15. Wieliczka DM, Weng S, Querry MR (1989) Wedge shaped cell for highly absorbent liquids: infrared optical constants of water. *Appl Opt* 28:1714–1719
16. El-Sherif AF, King TA (2003) Soft and hard tissue ablation with short-pulse high peak power and continuous thulium-silica fibre lasers. *Lasers Med Sci* 18:139–147
17. Kalaycioglu H, Sennaroglu A, Kurt A (2005) Influence of doping concentration on the power performance of diode-pumped continuous-wave Tm³⁺:YAlO₃ lasers. *IEEE J Sel Top Quan Electron* 11:667–673
18. Geldi C, Bozkulak O, Tabakoglu HO, Isci S, Kurt A, Gulsoy M (2006) Development of a surgical diode-lasers: controlling the mode of operation. *Photomed Laser Surg* 24:723–729
19. Ding Y, Ying H, Shao S (2000) A time-varying fuzzy on-off control system with application to the control of tissue temperature during laser heating. *IEEE Fuzzy Syst* 1:528–533
20. Birch JF, Mandley DJ, Williams SL, Worrall DR, Trotter PJ, Wilkinson F, Bell PR (2000) Methylene blue-based protein solder for vascular anastomoses: an in vitro burst pressure study. *Lasers Surg Med* 26:323–329
21. Pierce MC, Jackson SD, Dickinson MR, King TA (1999) Laser–tissue interaction with a high-power 2- μ m fiber laser: Preliminary studies with soft tissue. *Lasers Surg Med* 25:407–413
22. Lange BI, Brendel T, Hüttmann G (2002) Temperature dependence of light absorption in water at holium and thulium laser wavelengths. *Appl Opt* 41:5797–5803
23. Jansen ED, van Leeuwen TG, Motamedi M, Borst C, Welch AJ (2005) Temperature dependence of the absorption coefficient of water for midinfrared laser radiation. *Lasers Surg Med* 14:258–268
24. McDonald AV, Claffey NM, Pearson GJ, Blau W, Setchell DJ (2000) Effect of Nd:YAG radiation at millisecond pulse duration on dentine crater depth. *Lasers Surg Med* 27:213–223
25. Karamzadeh AM, Wong BJF, Crumley RL, Ahuja G (2004) Lasers in pediatric airway surgery: current and future clinical applications. *Lasers Surg Med* 35:128–134
26. Bilici T, Topaloglu N, Tabakoglu O, Kalaycioglu H, Kurt A, Sennaroglu A, Gulsoy M (2010) Modulated and continuous-wave operations of thulium (Tm:YAP) laser in tissue welding. *J Biomed Opt* 13:038001
27. Forss N, Raij TT, Sepp M, Hari R (2005) Common cortical network for first and second pain. *Neuroimage* 24:132–142